articles

molecular pharmaceutics

Biodistribution, Clearance, and Biocompatibility of Iron Oxide Magnetic Nanoparticles in Rats

Tapan K. Jain,[†] Maram K. Reddy,[†] Marco A. Morales,[‡] Diandra L. Leslie-Pelecky,[‡] and Vinod Labhasetwar*[,†,§]

Department of Biomedical Engineering, Lerner Research Institute, Cleveland Clinic, Cleveland, Ohio 44195, Department of Physics & Astronomy and Nebraska Center for Materials and Nanoscience, University of Nebraska−Lincoln, Lincoln, Nebraska 68588-0111, and Department of Pharmaceutical Sciences, College of Pharmacy, Nebraska Medical Center, Omaha, Nebraska 68198-6025

Received September 21, 2007; Revised Manuscript Received November 16, 2007; Accepted November 25, 2007

Abstract: It is essential to determine the biodistribution, clearance, and biocompatibility of magnetic nanoparticles (MNPs) for *in vivo* biomedical applications to ensure their safe clinical use. We have studied these aspects with our novel iron oxide MNP formulation, which can be used as a magnetic resonance imaging (MRI) agent and a drug carrier system. Changes in serum and tissue iron levels were analyzed over 3 weeks after intravenous administration of MNPs to rats. Serum alanine aminotransferase (ALT), aspartate aminotransferase (AST), alkaline phosphatase (AKP) levels, and total iron-binding capacity (TIBC) were also measured with time to assess the effect of MNPs on liver function. Selected tissues were also analyzed for oxidative stress and studied histologically to determine biocompatibility of MNPs. Serum iron levels gradually increased for up to 1 week but levels slowly declined thereafter. Biodistribution of iron in various body tissues changed with time but greater fraction of the injected iron localized in the liver and spleen than in the brain, heart, kidney, and lung. Magnetization measurements of the liver and spleen samples showed a steady decrease over 3 weeks, suggesting particle degradation. Serum showed a transient increase in ALT, AST, AKP levels, and TIBC over a period of 6−24 h following MNP injection. The increase in oxidative stress was tissue dependent, reaching a peak at ~3 days and then slowly declining thereafter. Histological analyses of liver, spleen, and kidney samples collected at 1 and 7 days showed no apparent abnormal changes. In conclusion, our MNPs did not cause long-term changes in the liver enzyme levels or induce oxidative stress and thus can be safely used for drug delivery and imaging applications.

Keywords: Imaging; MRI; drug delivery; oxidative stress; nanotoxicity

Introduction

Magnetic nanoparticles (MNPs) are explored for various biomedical applications such as targeted drug delivery,[1,2] cell sorting,[3] contrast agents for magnetic resonance imaging (MRI),[4,5] and hyperthermia.[6] The dual function of MNPs as imaging agents as well as carriers for drug delivery is complementary, as the detection of pathologies and effective drug delivery are critical components of successful therapy in many disease conditions. MNPs that can serve both purposes are of high clinical significance. We have developed an iron oxide MNP coated with both oleic acid (OA) and Pluronic (BASF Corp., Mt. Olive, NJ) that can be loaded with high doses of hydrophobic drugs (Figure 1).[7] An advantage of using MNPs for drug delivery applications over other nanocarriers (e.g., mi-

* To whom correspondence should be addressed. Mailing address: Department of Biomedical Engineering/ND20, Cleveland Clinic, 9500 Euclid Ave, Cleveland, Ohio 44195. Tel: 16/445-9364. Fax: 216/444-9198. E-mail: labhasv@ccf.org.

[†] Lerner Research Institute.

[‡] University of Nebraska−Lincoln.

[§] Nebraska Medical Center.

10.1021/mp7001285 CCC: $40.75
Published on Web 01/25/2008

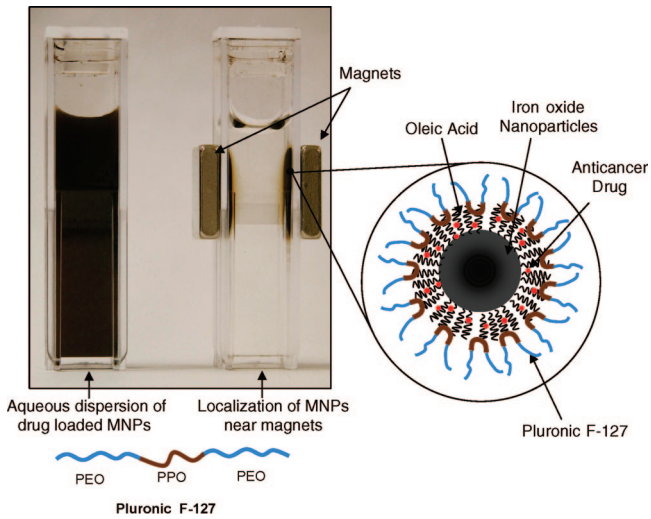

Figure 1. Schematic of oleic acid (OA)-Pluronic-coated iron oxide magnetic nanoparticles (MNPs). Hydrophobic drugs can be partitioned in the OA layer around the iron oxide core. Pluronic anchored onto OA provides aqueous dispersity. Figure modified from ref 7.

celles, polymeric nanoparticles, liposomes, etc.) is that their magnetic properties allow monitoring and quantitative determination of their biodistribution and thus, indirectly, that of the drug associated with MNPs (including their localization in the target tissue) using noninvasive MRI and magnetometry.[8] This is a crucial issue in drug therapy because failure to achieve the expected therapeutic outcome could be due to suboptimal dosing of the drug in the target tissue.[9] For example, in cancer chemotherapy, optimized dosing is critical not only for achieving tumor regression, but also to prevent the tumor from developing drug resistance and contributing to relapse.[10]

In addition to imaging and drug delivery, MNPs are being investigated using MRI to monitor the migration of particular cell populations in the body (e.g., progenitor cells or macrophages) that have been tagged with MNPs prior to injection in disease conditions.[11] MRI data can be a useful research tool to determine the targeting efficacy of ligands such as peptides or antibodies.[12] The suitability of MNPs has also been tested for other intracellular applications, such as for visualization of gene expression at the molecular level.[13]

It is essential to determine the biodistribution, clearance, and biocompatibility of MNPs that may be used for drug delivery and imaging applications *in vivo*. Biodistribution of MNPs depends on their properties such as surface characteristics, size, and shape,[14] which can affect particle-cell interactions and interactions with serum proteins (opsonization).[15] Other factors such as magnetic materials and their biodegradation products are important from the point of view of biocompatibility of MNPs.[16] Equally important is determining iron clearance as MNPs degrade since excessive tissue accumulation of free iron is known to cause toxicity.[17] In this paper, we have determined the biodistribution, clearance, and biocompatibility of our oleic acid−Pluronic-coated iron oxide MNP formulation.[7]

(1) Alexiou, C.; Arnold, W.; Klein, R. J.; Parak, F. G.; Hulin, P.; Bergemann, C.; Erhardt, W.; Wagenpfeil, S.; Lubbe, A. S. Locoregional cancer treatment with magnetic drug targeting. *Cancer Res.* **2000**, *60*, 6641–6648.

(2) Alexiou, C.; Jurgons, R.; Schmid, R. J.; Bergemann, C.; Henke, J.; Erhardt, W.; Huenges, E.; Parak, F. Magnetic drug targeting−biodistribution of the magnetic carrier and the chemotherapeutic agent mitoxantrone after locoregional cancer treatment. *J. Drug Target.* **2003**, *11*, 139–149.

(3) Clement, J. H.; Schwalbe, M.; Buske, N.; Wagner, K.; Schnabelrauch, M.; Gornert, P.; Kliche, K. O.; Pachmann, K.; Weitschies, W.; Hoffken, K. Differential interaction of magnetic nanoparticles with tumor cells and peripheral blood cells. *J. Cancer Res. Clin. Oncol.* **2006**, *132*, 287–292.

(4) Artemov, D. Molecular magnetic resonance imaging with targeted contrast agents. *J. Cell. Biochem.* **2003**, *90*, 518–524.

(5) Jung, C. W.; Jacobs, P. Physical and chemical properties of superparamagnetic iron oxide MR contrast agents: ferumoxides, ferumoxtran, ferumoxsil. *Magn. Reson. Imaging* **1995**, *13*, 661–674.

(6) Ito, A.; Tanaka, K.; Kondo, K.; Shinkai, M.; Honda, H.; Matsumoto, K.; Saida, T.; Kobayashi, T. Tumor regression by combined immunotherapy and hyperthermia using magnetic nanoparticles in an experimental subcutaneous murine melanoma. *Cancer Sci.* **2003**, *94*, 308–313.

(7) Jain, T. K.; Morales, M. A.; Sahoo, S. K.; Leslie-Pelecky, D. L.; Labhasetwar, V. Iron oxide nanoparticles for sustained delivery of anticancer agents. *Mol. Pharm.* **2005**, *2*, 194–205.

(8) Koning, G. A.; Krijger, G. C. Targeted multifunctional lipid-based nanocarriers for image-guided drug delivery. *Anticancer Agents Med. Chem.* **2007**, *7*, 425–440.

(9) Broxterman, H. J.; Lankelma, J.; Hoekman, K. Resistance to cytotoxic and anti-angiogenic anticancer agents: similarities and differences. *Drug Resist. Updat.* **2003**, *6*, 111–127.

(10) Bezwoda, W. R. High-dose chemotherapy with hematopoietic rescue in breast cancer: from theory to practice. *Cancer Chemother. Pharmacol.* **1997**, *40*, S79–S87.

(11) Frank, J. A.; Miller, B. R.; Arbab, A. S.; Zywicke, H. A.; Jordan, E. K.; Lewis, B. K.; Bryant, L. H. Jr.; Bulte, J. W. M. Clinically Applicable Labeling of Mammalian and Stem Cells by Combining Superparamagnetic Iron Oxides and Transfection Agents. *Radiology* **2003**, *228*, 480–487.

(12) Gupta, A. K.; Naregalkar, R. R.; Vaidya, V. D.; Gupta, M. Recent advances on surface engineering of magnetic iron oxide nanoparticles and their biomedical applications. *Nanomed.* **2007**, *2*, 23–39.

(13) Weissleder, R.; Moore, A.; Mahmood, U.; Bhorade, R.; Benveniste, H.; Chiocca, E. A.; Basilion, J. P. In vivo magnetic resonance imaging of transgene expression. *Nat. Med.* **2000**, *6*, 351–355.

(14) Chouly, C.; Pouliquen, D.; Lucet, I.; Jeune, J. J.; Jallet, P. Development of superparamagnetic nanoparticles for MRI: effect of particle size, charge and surface nature on biodistribution. *J. Microencapsul.* **1996**, *13*, 245–255.

(15) Owens, D. E.; Peppas, N. A. Opsonization, biodistribution, and pharmacokinetics of polymeric nanoparticles. *Int. J. Pharm.* **2006**, *307*, 93–102.

(16) Gupta, A. K.; Gupta, M. Synthesis and surface engineering of iron oxide nanoparticles for biomedical applications. *Biomaterials* **2005**, *26*, 3995–4021.

(17) Weir, M. P.; Gibson, J. F.; Peters, T. J. Haemosiderin and tissue damage. *Cell Biochem. Funct.* **1984**, *2*, 186–194.

Experimental Section

Iron(III) chloride hexahydrate ($FeCl_3 \cdot 6H_2O$) (Fe(III)) pure granulated 99%, iron(II) chloride tetrahydrate ($FeCl_2 \cdot 4H_2O$) (Fe(II)) 99+%, ammonium hydroxide (5 M), and oleic acid (OA) were purchased from Fisher Scientific (Pittsburgh, PA). Pluronic F-127 was received as a gift from BASF Corp. (Mt. Olive, NJ). Polyvinyl alcohol (PVA, average MW 30000–70000), paraformaldehyde, and Mohr's salt were obtained from Sigma-Aldrich (St. Louis, MO). Poly (D,L-lactide *co*-glycolide) (PLGA) 50:50 (inherent viscosity 1.32 dL/g) was purchased from Birmingham Polymers, Inc. (Birmingham, AL). Deionized water freshly purged with nitrogen gas was used in all the steps involved in the synthesis and formulation of MNPs.

Formulation of MNPs. Formulation of OA−Pluronic-coated iron oxide MNPs was prepared according to our previously described procedure.[7] In brief, aqueous solutions of 0.1 M Fe(III) (30 mL) and 0.1 M Fe(II) (15 mL) were mixed to which 3 mL of 5 M ammonium hydroxide solution was added to form iron oxide nanoparticles. To the above preparation, 100 mg of OA was added and heated for 30 min to 80 °C with stirring to evaporate ammonia. The content was cooled to room temperature, and the black precipitate thus obtained was washed twice with 15 mL of deionized water to remove excess OA. To the precipitate was added 45 mL of deionized water, followed by 100 mg of Pluronic. The suspension was stirred overnight in a closed container to minimize exposure to atmospheric oxygen to prevent oxidation of iron oxide nanoparticles. The particles were separated using neodymium iron boron magnets (12200 G; Edmund Scientific, Tonawanda, NY), redispersed, and washed three times with water to remove soluble salts and excess Pluronic; particles were separated during each washing step using magnets as described above. The particles were redispersed in 15 mL of water by sonication in a water-bath sonicator (FS-30, Fisher Scientific) for 10 min and centrifuged at 1000 rpm for 20 min at 7–11 °C to remove any large aggregates. The supernatant containing OA−Pluronic-stabilized MNPs was collected and further concentrated using magnetic separation as described above. The mean hydrodynamic diameter of MNPs was 193 nm (polydispersity index = 0.262) and ζ-potential of −0.22 mV. The core diameter of iron oxide particles as measured by transmission electron microscopy was 11 ± 2 nm. As discussed in our previous study, OA and Pluronic coatings around the iron oxide core contribute toward the hydrodynamic diameter of MNPs.[7]

Determination of Iron Oxide and Iron Content in Nanoparticle Formulation. The concentration of iron oxide in the preparation was determined by lyophilizing a portion of the sample in a preweighed vial. The amount of OA and Pluronic associated with particles was determined by thermogravimetric analysis. This value was then subtracted from the total weight of the formulation to determine the iron oxide content. The iron levels in the formulation were determined using the 1,10-phenanthroline colorimetric method.[18] To 0.5 mg of lyophilized samples, 200 μL of concentrated hydrochloric acid (HCl) was added and incubated for 1 h at 25 °C. The sample was then diluted to 1 mL with water. To 50 μL of aliquot was added 2 mL of 0.5 M ammonium acetate−acetic acid buffer, pH 3.0, followed by 100 μL of 10% aqueous solution of hydroxylamine hydrochloride to reduce Fe(III) to Fe(II). To this solution was added 500 μL of 0.3% aqueous solution of 1,10 phenanthroline (Sigma-Aldrich), and the solution was incubated for 1 h at room temperature. The absorbance was measured at 511 nm using a spectrophotometer (UV-1601PC, UV–vis spectrophotometer, Shimadzu Scientific Instruments, Inc., Columbia, MD). The concentration of iron in the samples was calculated from a standard plot, which was prepared using Mohr's salt solution in 0.01 N HCl in the concentration range of 0.5–4.0 μg of Fe/mL. In addition to the iron content, each batch of MNP formulation was characterized for particle size using transmission electron microscopy and dynamic light scattering to ensure their dispersion in aqueous solution.

Formulation of PLGA Nanoparticles and OA-Pluronic Emulsion. PLGA nanoparticles were used as a model biocompatible formulation at the same dose (w/w) as MNPs to determine whether the changes seen in the liver enzymes were specific to MNPs or a general response to the particulate injection. PLGA nanoparticles were prepared by a solvent evaporation method as previously described.[19] In a typical procedure, 90 mg of PLGA was dissolved in 3 mL of chloroform, which was then emulsified in 12 mL of (2% w/v) PVA solution using sonication. This emulsion was stirred overnight to evaporate chloroform, thereby forming nanoparticles that were recovered by ultracentrifugation, washed, and lyophilized. Similarly, OA−Pluronic emulsion (without iron oxide particles) was used as a control to determine whether the effect on liver enzymes was due to nanoparticles or the formulation components (i.e., OA or Pluronic). The amount of OA and Pluronic associated with nanoparticles was calculated as per our previously described protocol.[7] Based on that, 6 mg of OA was emulsified in an aqueous solution of Pluronic (5.7 mg/2.0 mL of saline) by sonication in a water bath sonicator for 20 min at room temperature. The mean diameter of droplet size measured using dynamic light scattering (NICOMP 380 ZLS, Zeta Potential/ Particle Sizer, Santa Barbara, CA) was 86.2 nm (polydispersity index = 0.18). A 1 mL/kg aliquot of the emulsion was injected intravenously to rats which contained the same dose of OA and Pluronic that is associated with the dose of MNPs injected.

***In Vivo* Studies.** Male Sprague–Dawley rats (240–260 g, Charles River Laboratories, Wilmington, MA) were used in this experiment. All of the procedures complied with the standards for humane care and use of animal subjects as

(18) Jeffery, G. H.; Bassett, J.; Mendham, J. Denny, R. C. *Vogel's Text Book of Quantitative Chemical Analysis*, 5th ed.; John Wiley & Sons, Inc.: New York, 1989; pp 690−692.

(19) Davda, J.; Labhasetwar, V. Characterization of nanoparticle uptake by endothelial cells. *Int. J. Pharm.* **2002**, *233*, 51–59.

stated in the Guide for the Care and Use of Laboratory Animals (Institute of Laboratory Resources, National Academy of Sciences, Bethesda, MD) and animal welfare policy of the University of Nebraska Medical Center. Rats were anesthetized with an intraperitoneal injection of ketamine (80 mg/kg) and xylazine (10 mg/kg) mixture. A suspension of MNPs (10 mg Fe/mL) was prepared in saline and injected slowly through the tail vein at a dose of 10 mg Fe/kg. Control experiments were carried out with and without injecting saline to determine if the injection itself caused any changes in liver enzyme levels. Animals were allowed to recover following nanoparticle injection. At different time points, animals were euthanized with an intraperitoneal injection of pentobarbital sodium (120 mg/kg), and ~4 mL of blood was immediately collected through a cardiac puncture. Animals were then perfused transcardially with heparinized saline for 20 min, and various tissues (liver, spleen, kidney, heart, lung, and brain) were collected, washed thoroughly with saline, and stored at −80 °C until taken for analysis. These tissues were used for determination of iron content and for lipid peroxidation using a lipid hydroperoxide (LHPO) assay. In animals from which tissues were collected for histological examination, a 4% paraformaldehyde solution which was prepared by dissolving paraformaldehyde (Sigma-Aldrich) in near-boiling phosphate-buffered saline (PBS, 154 mM, pH = 7.4) was perfused for 2 min following the saline perfusion as described above.

Analysis of Serum. Blood samples were allowed to clot at room temperature and centrifuged at 1500*g* for 10 min to separate the serum for collection. The serum samples were immediately sent to the Clinical Core Laboratory for analysis of ALT, AST, and AKP levels. In addition, serum samples were analyzed at the Core for iron levels and total iron binding capacity (TIBC). TIBC represents the amount of iron in the blood that would be present if the total transferrin in plasma were saturated. Since transferrin is produced in the liver, it was used to indirectly indicate liver function.

Analysis of Tissue. Upon procurement of tissue, the wet weight of each sample was recorded. Tissue samples were then homogenized with a Tissue Tearor homogenizer (Model No. 985370, Biospec Products Inc., Bartlesville, OK) in nitrogen-purged water (~20% tissue wet weight) in an ice bath. The total volume of each homogenate was measured. Tissue homogenates were used to determine iron content and for the LHPO assay. To determine iron levels in tissues, 1 mL of each tissue homogenate was lyophilized in a test tube for 2 days at −60 °C and 7 μmHg vacuum (Lyph-Lock 12 Labconco, Kansas City, MO); weight of the tissue was determined by comparing the difference in weight of the empty tubes and that after lyophilization of the tissue. To each dry tissue sample was added 2 mL of 6 N HCl, the tubes were placed in a closed glass container, and the samples were heated overnight in an incubator set at 55 °C. Each sample was vortexed and centrifuged at 1000 rpm for 15 min (RT 7 Centrifuge, Sorvall, DuPont, CT), and 1 mL of the supernatant from each sample was collected in a separate test tube. Samples were dried under a stream of nitrogen gas. To each residue was added 1 mL of 0.01 N HCl, and the mixture was vortexed and centrifuged at 1000 rpm for 15 min. The resulting supernatant solution was diluted 50 times and analyzed using inductively coupled plasma-mass spectrometry (ICP-MS; Varian 800-MS, Palo Alto, CA). A stock solution of Fe was prepared using Mohr's salt in 0.01 N HCl. Suitable dilutions of the stock solution were prepared in 0.01 N HCl to obtain a standard plot in the range of 50–1000 parts per billion with respect to Fe. Samples having higher concentration outside the calibration curves were appropriately diluted. ^{57}Fe isotope counts were used to analyze the Fe content. From the weight of the tissue and volume of homogenate, iron levels were normalized to amount per gram wet weight of tissue. The fraction of the injected dose in each tissue at different time points was calculated from the total iron content in each tissue, from which the endogenous iron content for the respective tissue from control animals (saline injected) was subtracted.

Magnetic Susceptibility. Tissue samples from liver, spleen, and kidney were used for magnetic susceptibility measurements as these tissues showed higher iron levels than other tissues analyzed. Each powdered tissue sample (3–6 mg) prepared following homogenization and lyophilization was sealed along with 2–4 mg of paraffin wax (Sigma-Aldrich) in polyethylene bags. The bags were heated in a water bath at 70 °C to melt the paraffin, which produced homogeneously dispersed tissue powder in solid paraffin after the samples cooled to room temperature. Magnetization versus field measurements, M(H), were performed using an alternating gradient force magnetometer (Model Micromag 2900, Princeton Measurements Corporation, Princeton, NJ). Measurements were carried out at room temperature with a maximum applied magnetic field of 1.2 T. The magnetization data were normalized to the iron content as determined by ICP-MS. Analysis of the normalized data was performed by fitting the curves to a combination of a superparamagnetic (Langevin function) plus a diamagnetic (linear) function.[20,21]

Oxidative Stress Analysis. The change in the lipid hydroperoxide (LHPO) levels in different tissues with time was used as a biochemical marker to assess the effect of injected MNPs on oxidative stress using a lipid peroxidation assay kit (Cayman Chemical Co., Ann Arbor, MI).[22] Lipid hydroperoxides were extracted from each tissue homogenate (prepared as above) into chloroform as per the instructions provided with the assay kit. Typically, 0.5 mL of tissue homogenate was mixed with 0.5 mL of saturated methanolic solution of Extract R (a component of the kit) by vortexing,

(20) Stearns, M. B.; Cheng, Y. Determination of para- and ferromagnetic components of magnetization and magnetoresistance of granular Co/Ag films. *J. Appl. Phys.* **1994**, *75*, 6894–6899.

(21) Noyau, R. H.; Middleton, B. K.; Miles, J. J.; Mackintosh, N. D. Modelling digital recording in thin film media. *IEEE Trans. Magn.* **1988**, *24*, 2494–2496.

(22) Mihaljevic, B.; Katusin-Razem, B.; Razem, D. The reevaluation of the ferric thiocyanate assay for lipid hydroperoxides with special considerations of the mechanistic aspects of the response. *Free Radic. Biol. Med.* **1996**, *21*, 53–63.

to which 1 mL of cold chloroform was added and mixed thoroughly again by vortexing. This mixture was centrifuged at 1500*g* for 5 min at 0 °C to separate it into two layers; the chloroform layer (~700 μL) from the bottom of the tube was collected carefully and stored in an ice bath until taken for analysis. To 200 μL of the chloroform layer collected as above, 950 μL of chloroform-methanol (2:1 v:v) mixture was added, followed by 50 μL of chromogen (provided in the kit). Each sample was incubated at room temperature for 5 min, and the absorbance was measured at 500 nm using a UV/vis spectrophotometer. A standard plot of LHPO provided with the assay kit was prepared similarly, in the concentration range of 0.5−5.0 nM.

Histology. Portions of kidney, liver, and spleen were fixed in 10% buffered formalin−saline (Sigma-Aldrich) at 4 °C overnight and then embedded in paraffin blocks. Tissue sections of 5 μm thickness were stained with hematoxylin and eosin (H&E). The morphology of the tissue was observed under a microscope (Nikon Eclipse E600, Nikon Inc., Melville, NY) at 10× and 40× magnification.

Statistical Analysis. Student's *t*-test (two tailed, unpaired) was performed between nanoparticle groups vs saline controls, and *p* values less than 0.05 were considered statistically significant.

Results

Serum Iron Levels and Biodistribution of Iron. The serum iron level first increased over a period of 1 week and then declined slowly thereafter but remained higher than the saline control, suggesting that more than 3 weeks are required for the iron levels to return to normal (Figure 2a). There was no significant change in the TIBC of the serum following MNP injection (Figure 2b).

Changes in iron levels varied from tissue to tissue. Iron levels in the liver peaked at 6 h, the first data point after injection, and then gradually declined over the next 3 days prior to a slow increase after 7 days (Figure 3). Other tissues also experienced increased iron levels 1 week after the MNP injection, but this increase was relatively greater in liver, spleen, heart, and brain than in lung and kidney tissues (Figure 3). Biodistribution analysis showed that about 55% of the injected iron localized in the liver at 6 h but then was reduced to about 20% after 1 day. The other tissues demonstrated insignificant changes in iron levels during the first 24 h following MNP injection. However, at 3 weeks following particle injection, iron levels in the liver corresponded to ~50% of the injected dose and ~25% in the spleen, respectively. The fraction of the dose localized in other tissues was significantly lower compared to that localized in liver and spleen.

The magnetic susceptibility measurements of liver and spleen samples showed a gradual decrease in saturation magnetization over 3 weeks (Figure 4). Magnetization measurements are shown per gram of Fe, which may include iron sources other than the MNPs. The maximum magnetization of free MNPs at room temperature was 61 emu/g Fe_3O_4,[7]

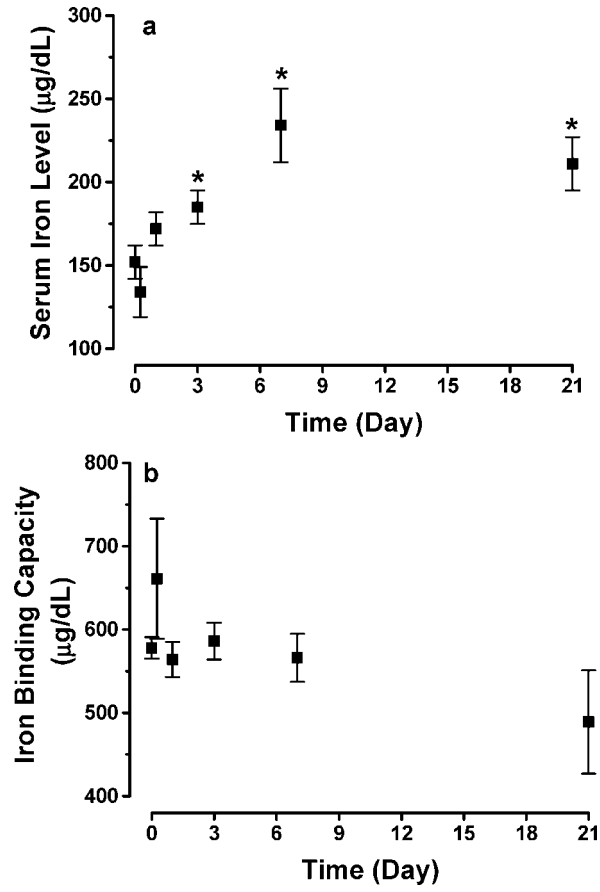

Figure 2. Changes in serum (a) iron levels and (b) total iron-binding capacity (TIBC) with time following a single-dose intravenous injection of MNPs to rats (10 mg of Fe/kg dose in 100 μL of saline). Data presented as mean ± sem (n = 4–8). *p < 0.05 vs saline control. Data at time point 0 was taken by injecting saline and sacrificing rats after 24 h.

which corresponds to 253 emu/g Fe. After 6 h, the maximum magnetization of the superparamagnetic component in the liver (averaged over the four samples) was about one-fourth that of free MNPs when normalized to iron content. Kidney samples showed markedly lower overall magnetizations, which could be due to lower accumulation of MNPs in that tissue.

Effect of MNPs on Liver Function. Changes in the serum AST, ALT, and AKP levels are commonly used as biochemical markers for liver function. The initial preliminary studies determined the enzyme activities at 24 h following particle injection. In the first set of experiments, the effect of injected MNPs on serum enzyme levels was compared with levels in control animals that had been euthanized without receiving any injection. There was a significant increase in AST activity (317 ± 31 U/L) in the MNP group than in control animals (154 ± 6 U/L) (Figure 5); therefore, we studied the effect of PLGA-nanoparticles as a representative biocompatible formulation to determine whether the response seen with MNPs was specific to these nanoparticles or a general response to particulate injection. We also injected an OA−Pluronic emulsion to determine whether the effect

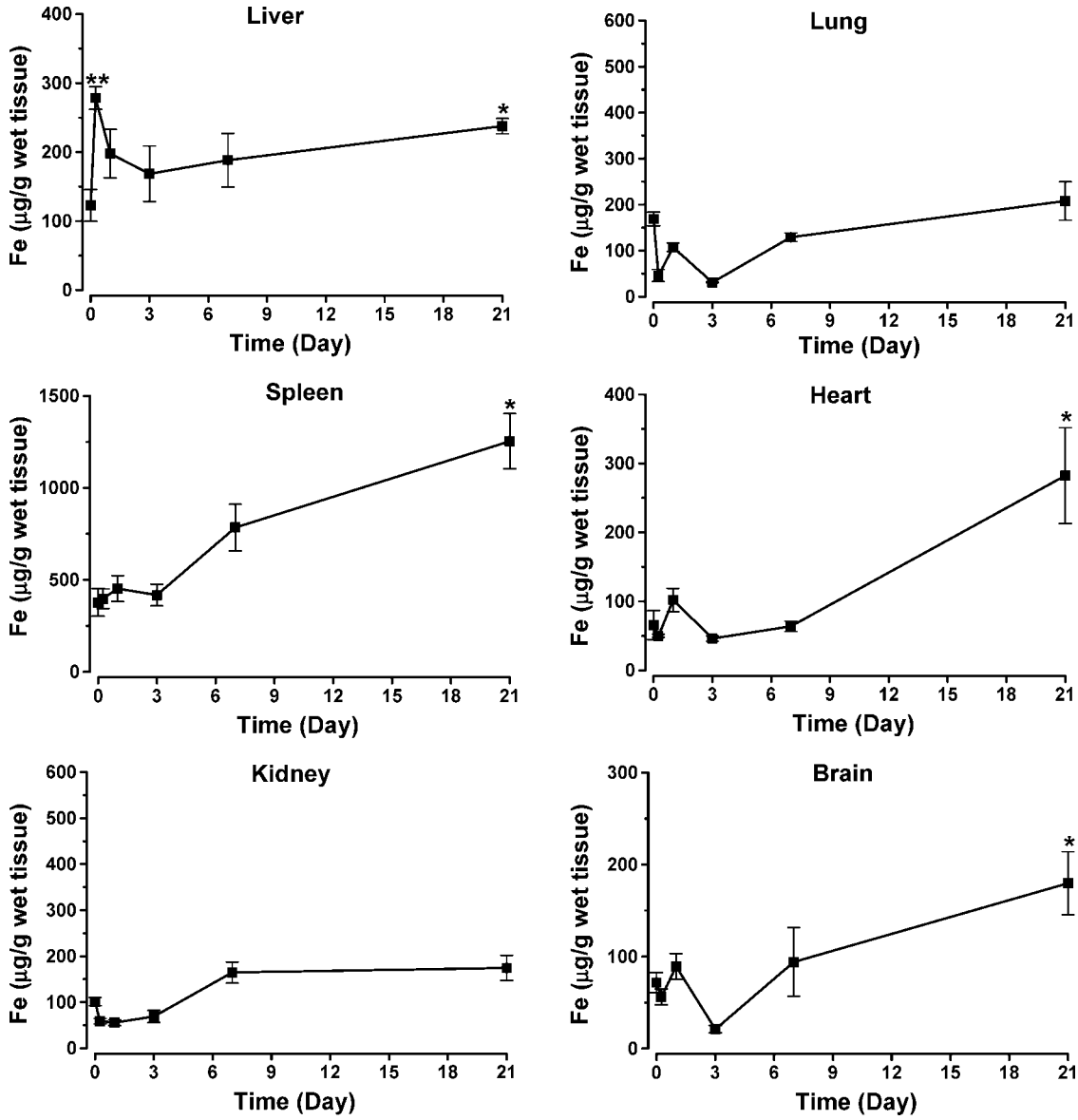

Figure 3. Changes in iron levels in different tissues following intravenous injection of MNPs. The injected dose of iron was 10 mg of Fe/kg in 100 μL of saline. Data presented as mean ± sem ($n = 4$). *$p < 0.05$ or **$p < 0.005$ vs saline control.

was due to the components (OA or Pluronic) used in the MNP formulation. Saline injection was used as a control in this set of experiments. Animals given a saline injection also showed a significant increase in serum AST activity (276 ± 22 U/L) compared to that in control animals, which received no injection. Further, the increase in AST activity in the saline control was almost the same as that seen in the MNP or PLGA-nanoparticle groups (Figure 5). Saline was used as a control in subsequent studies to determine the change in enzyme activity with time after MNP injection. There was a slight but transient increase in the AST, ALT, and AKP levels as compared to the saline control; however, the levels returned to normal within 3 days post injection (Figure 6).

Effect of MNPs on Oxidative Stress and Histological Analysis. LHPO levels in liver, spleen, and kidney increased, reaching a peak at about 3 days following MNP injection (Figure 7). The response was tissue dependent, with liver demonstrating a marginal increase and returning to normal values within 1 week, whereas the kidney and spleen took 3 weeks to return to normal values. No significant changes in LHPO levels were observed for lung, brain, and heart tissues (Figure 7). Histological analysis of the liver, spleen, and kidney did not show any apparent change in the cellular structures at 1 day (data not shown) or 7 days following MNP injection (Figure 8).

Discussion

Most formulations of MNPs use dextran or starch as a stabilizing agent to form a water-dispersible system,[23] with

(23) LaConte, L.; Nitin, N.; Bao, G. Magnetic nanoparticle probes. *Mater. Today* **2005**, *8*, 32–38.

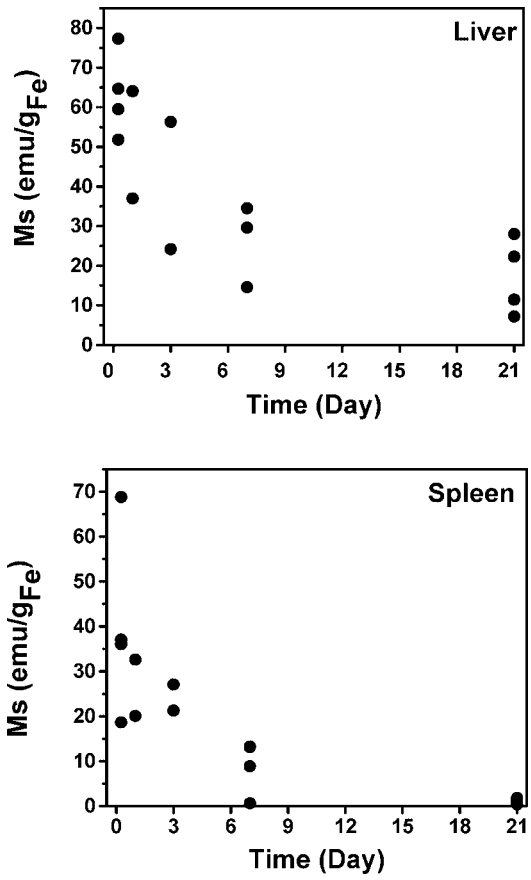

Figure 4. Change in the saturation magnetization of liver and spleen tissue samples vs time after injection of MNPs. Error bars are smaller than the symbol size. The first data point represents magnetization values at 6 h after MNP injection. The maximum magnetization of free MNPs (prior to injection) was 253 emu/g Fe.

the drug of interest conjugated to the outer layer of MNPs. Apart from the complexity of conjugation chemistry, the drug-loading capacity of these MNPs is low, and the conjugated drug is released within hours.[1] These factors limit the applications of MNPs as drug-carrier systems because the conjugated drug could be released before localizing in the target tissue. With our MNPs, the drug can be loaded at high concentration in the OA layer surrounding the magnetic core, and the loaded drug is released over a period of weeks.[7]

The present study was designed to determine the biodistribution, clearance, and biocompatibility of our MNP formulation, as size, shape, and surface properties could significantly influence the above *in vivo* properties of MNPs. Since our formulation has a unique combination of OA and Pluronic coatings, we anticipated that these MNPs would show different biodistribution characteristics than previously known for starch or dextran-coated MNPs. We also determined the clearance of iron, considering that excessive accumulation of iron in the body could be of concern as free iron is known to cause oxidative stress.[24] Hence, we determined the effect of injected MNPs on oxidative stress in different tissues as well as the changes in the liver enzymes as a measure of the liver function. Data obtained from these studies should help us to further optimize the formulation, if necessary, and to enhance the efficiency of our MNPs for imaging and drug delivery applications.

We observed a gradual increase in the serum iron level for 1 week prior to a slow decline, indicating that clearance of the MNPs requires more than 3 weeks (Figure 2a). The serum iron level is perhaps the result of several simultaneously occurring processes, such as degradation of injected iron particles, the iron's subsequent binding to different serum proteins (e.g., transferrin), redistribution of the bound iron to cells and tissue, and its elimination. Our serum iron data do not discriminate between bound and free forms of iron, but it appears that most of the iron in the body is in the bound form because of its slow clearance kinetics. Bourrinet et al.[25] in their study with Fe-Ferumoxtran-10 (Advanced Magnetics, Cambridge, MA), which is an iron oxide core coated with low molecular weight dextran, have reported slow clearance of iron, extending beyond 7 weeks. Iron can become incorporated into the body's iron store and progressively into the red blood cells (hemoglobin), thus slowing the clearance of iron. The authors reported elimination of 18–22% of injected iron through urine and feces in different animal species during 7 weeks; however, a few other studies have reported more rapid clearance of the injected iron (25% in 19 days).[26] This discrepancy in clearance time could have been due to the difference in the size of the iron oxide core particle and/or the coating material, both of which can affect the degradation and biodistribution of MNPs.

MNPs initially are superparamagnetic, while free iron is expected to be paramagnetic. The saturation magnetization of the superparamagnetic component of the magnetization decreases with MNP size, suggesting that MNPs degraded over the 3-week period studied, or that MNPs are eliminated from the tissues. The biodistribution data demonstrated that about 55% of the injected dose of iron localized in the liver at 6 h following particle injection, which appears to be due to clearance of the MNPs by the reticuloendothelial system (RES). RES clearance of particles depends upon several factors, including particle size, shape, and surface properties. The mean particle size of our MNPs measured using transmission electron microscopy was 11 ± 2 nm, and the hydrodynamic diameter was 193 nm based on laser light

(24) McCord, J. M. Effects of positive iron status at a cellular level. *Nutr. Rev.* **1996**, *54*, 85–88.

(25) Bourrinet, P.; Bengele, H. H.; Bonnemain, B.; Dencausse, A.; Idee, J. M.; Jacobs, P. M.; Lewis, J. M. Preclinical safety and pharmacokinetic profile of ferumoxtran-10, an ultrasmall superparamagnetic iron oxide magnetic resonance contrast agent. *Invest. Radiol.* **2006**, *41*, 313–324.

(26) Weissleder, R.; Stark, D. D.; Engelstad, B. L.; Bacon, B. R.; Compton, C. C.; White, D. L.; Jacobs, P.; Lewis, J. Superparamagnetic iron oxide: pharmacokinetics and toxicity. *Am. J. Roentgenol.* **1989**, *152*, 167–173.

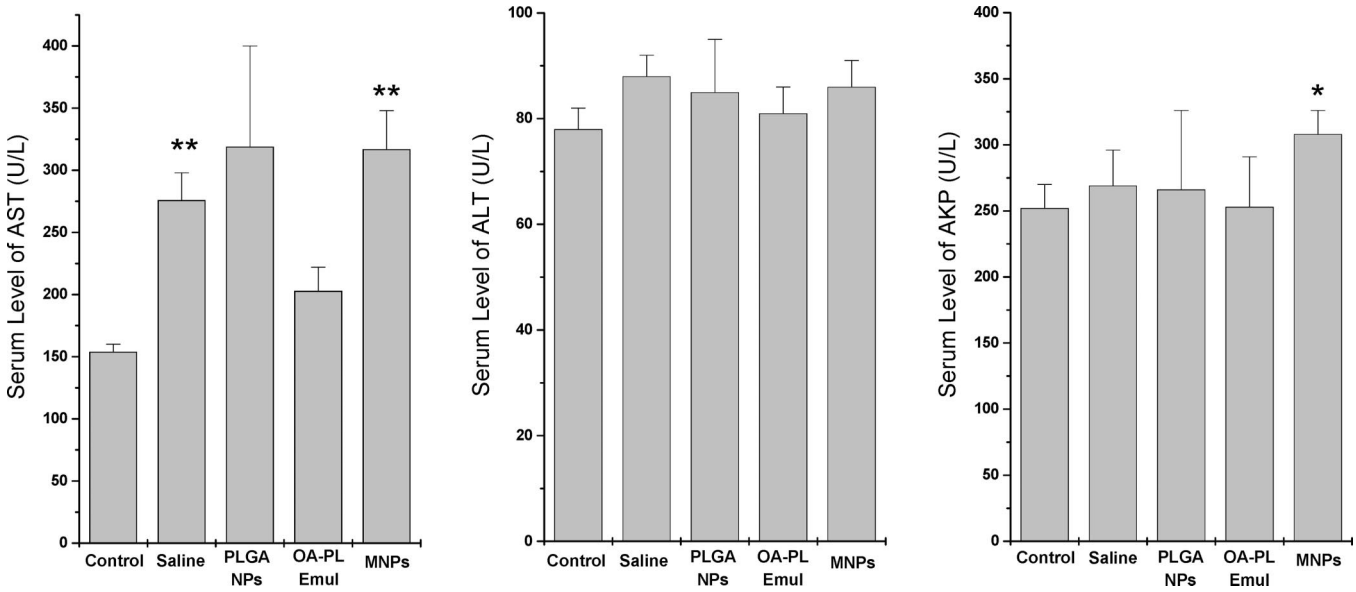

Figure 5. Changes in levels of serum (a) aspartate aminotransferase (AST), (b) alanine aminotransferase (ALT), and (c) alkaline phosphatase (AKP) at 24 h following saline, OA-Pluronic emulsion, PLGA-nanoparticles, and MNP injection. Ketamine/xylazine (K/X) was injected intraperitoneally to anesthetize rats before injection of formulations. (Control: no saline injection and no K/X administration.) Data presented as mean ± sem (n = 4–8). *p < 0.05, **p < 0.005 with respect to control.

scattering measurement.[7] Neuberger et al.[27] have reported that larger-sized nanoparticles are eliminated from the bloodstream faster than smaller-sized nanoparticles. It has also been demonstrated that for particles smaller than 40 nm in diameter, both biodistribution and blood half-life of the iron oxide particles are determined by the coating material rather than the mean hydrated particle size.[28] Our formulation is coated with OA and Pluronic that contribute toward the increase in hydrodynamic diameter of the iron oxide core. We therefore speculate that the initial high levels of iron observed in the liver may be due to the uptake of MNPs by the liver via the first-pass effect because of the increased diameter of MNPs. Okon et el.[29] have reported uptake of the major fraction of injected dextran-coated iron oxide MNPs by the Küpffer cells. Many other studies have reported greater than 75% uptake of MNPs by the RES, particularly by the liver.[14] Relatively lower uptake of our MNPs by the liver could be partly due to the coating with Pluronic, which is known to inhibit opsonization of injected particles.[30] We have used Pluronic F-127 in this study to stabilize the MNPs, but it is known that the ratio of hydrophilic polyethylene oxide (PEO) and hydrophobic polypropylene oxide (PPO) segments in Pluronic influence the interactions of particles with serum protein and hence their systemic circulation time. Other Pluronic types, particularly F-108 and T-908[30] or polyethylene glycol (molecular weight ~5,000),[31] are known to minimize the opsonization of colloidal particles and hence their clearance by the RES. Therefore, it would be interesting to determine the effect of these surface modifications on biodistribution of MNPs in future studies.

In addition to size, the charge of MNPs also influences the uptake of MNPs by the liver. Our particles have a ζ potential of −0.22 mV, which is almost neutral. Chouly et al.,[14] in their study of dextran-coated nanoparticles, reported that the liver's uptake of charged particles is greater than neutral particles. Therefore, the almost neutral charge of our MNPs is an advantage in preventing their rapid clearance from the circulation. MNPs with a prolonged blood half-life could be useful in the imaging of several pathological conditions, such as metastatic lymph node, inflammatory, and/or degenerative diseases. In addition, it can be used as blood pool agents for angiography and for determining tumor

(27) Neuberger, T.; Schopf, B.; Hofmann, H.; Hofmann, M.; von Rechenberg, B. Superparamagnetic nanoparticles for biomedical applications: Possibilities and limitations of a new drug delivery system. *J. Magn. Magn. Mater.* **2005**, *293*, 483–496.

(28) Briley-Saebo, K.; Bjornerud, A.; Grant, D.; Ahlstrom, H.; Berg, T.; Kindberg, G. M. Hepatic cellular distribution and degradation of iron oxide nanoparticles following single intravenous injection in rats: implications for magnetic resonance imaging. *Cell Tissue Res.* **2004**, *316*, 315–323.

(29) Okon, E.; Pouliquen, D.; Okon, P.; Kovaleva, Z. V.; Stepanova, T. P.; Lavit, S. G.; Kudryavtsev, B. N.; Jallet, P. Biodegradation of magnetite dextran nanoparticles in the rat. A histologic and biophysical study. *Lab. Invest.* **1994**, *71*, 895–903.

(30) Tan, J. S.; Butterfield, D. E.; Voycheck, C. L.; Caldwell, K. D.; Li, J. T. Surface modification of nanoparticles by PEO/PPO block copolymers to minimize interactions with blood components and prolong blood circulation in rats. *Biomaterials* **1993**, *14*, 823–833.

(31) Moghimi, S. M.; Szebeni, J. Stealth liposomes and long circulating nanoparticles: critical issues in pharmacokinetics, opsonization and protein-binding properties. *Prog. Lipid Res.* **2003**, *42*, 463–478.

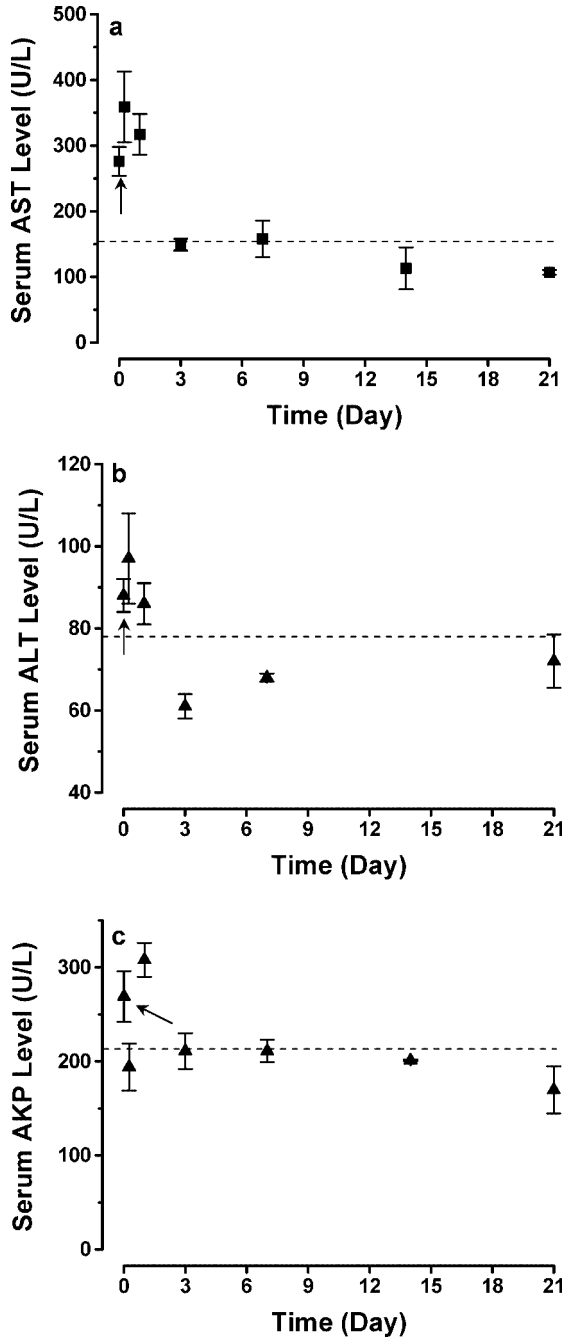

Figure 6. Changes in serum liver enzyme levels with time following a single-dose intravenous injection of MNPs in rats (10 mg Fe/kg dose in 100 μL of saline): (a) aspartate aminotransferase (AST), (b) alanine aminotransferase (ALT), and (c) alkaline phosphatase (AKP). Dashed line in each graph represents control values (i.e., no K/X and no saline injected). Data presented as mean $\pm$ sem ($n = 4$). Data at time point 0 is saline control (represented by arrows).

permeability and tumor blood volume, cerebral blood volume, and vessel size index measurements.[32]

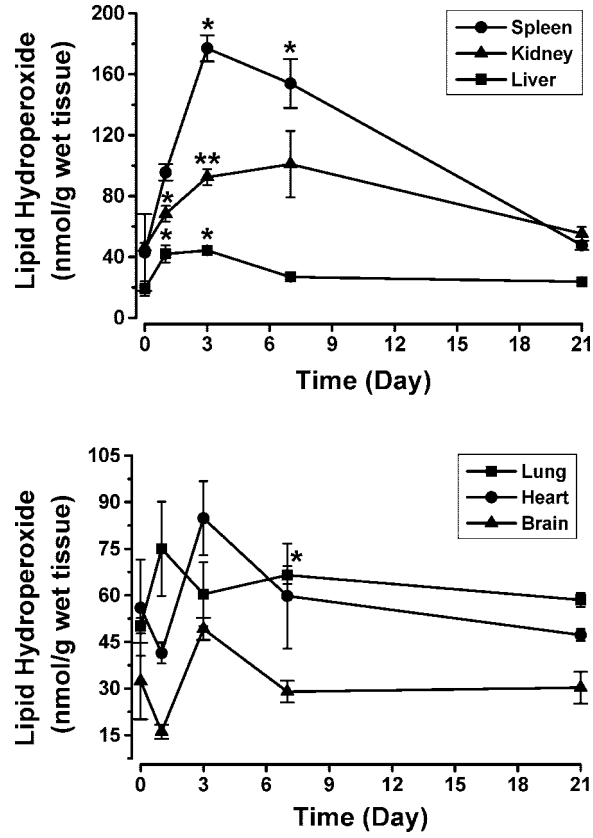

Figure 7. Changes in lipid hydroperoxide (LHPO) levels as a measure of oxidative stress in different tissues with time following injection of MNPs in rats (10 mg Fe/kg dose in 100 μL of saline). Data presented as mean $\pm$ sem ($n = 4$).

The MNPs have differential organ distribution patterns that vary with time and seem to be influenced by several factors besides the RES. The magnetic measurements of the liver and the spleen samples suggest the loss of magnetization over a period of 1 week (Figure 4). This loss could also be due to biodegradation of superparamagnetic nanoparticles to iron metabolites or free iron, neither of which should be superparamagnetic. There was variation in magnetization values of the tissue collected from different animals, which could be due to the heterogeneous distribution of MNPs in the organ. Perhaps, homogenizing the entire organ prior to taking samples for measurement could give more consistent data. It has been suggested that the Küpffer cells in liver can degrade iron oxide nanoparticles and can incorporate most of the iron into ferritin.[28] The incorporation of iron into ferritin could change the magnitude of the superparamagnetic component, as ferritin is superparamagnetic at room temperature. The loss of magnetization in 1 week with our MNPs also is consistent with the degradation of dextran-coated iron oxide MNPs in the lysosomal compartment of the macrophage.[33] Okano et al.[29] examined the biodegradation of magnetite-dextran nanoparticles in rats and reported a sharp decrease in magnetic susceptibility at day 3, followed by a gradual decrease thereafter until day 14. In contrast, our results show a steady decrease in the saturation magnetization.

(32) Corot, C.; Robert, P.; Idee, J.-M.; Port, M. Recent advances in iron oxide nanocrystal technology for medical imaging. *Adv. Drug Deliv. Rev.* **2006**, *58*, 1471–1504.

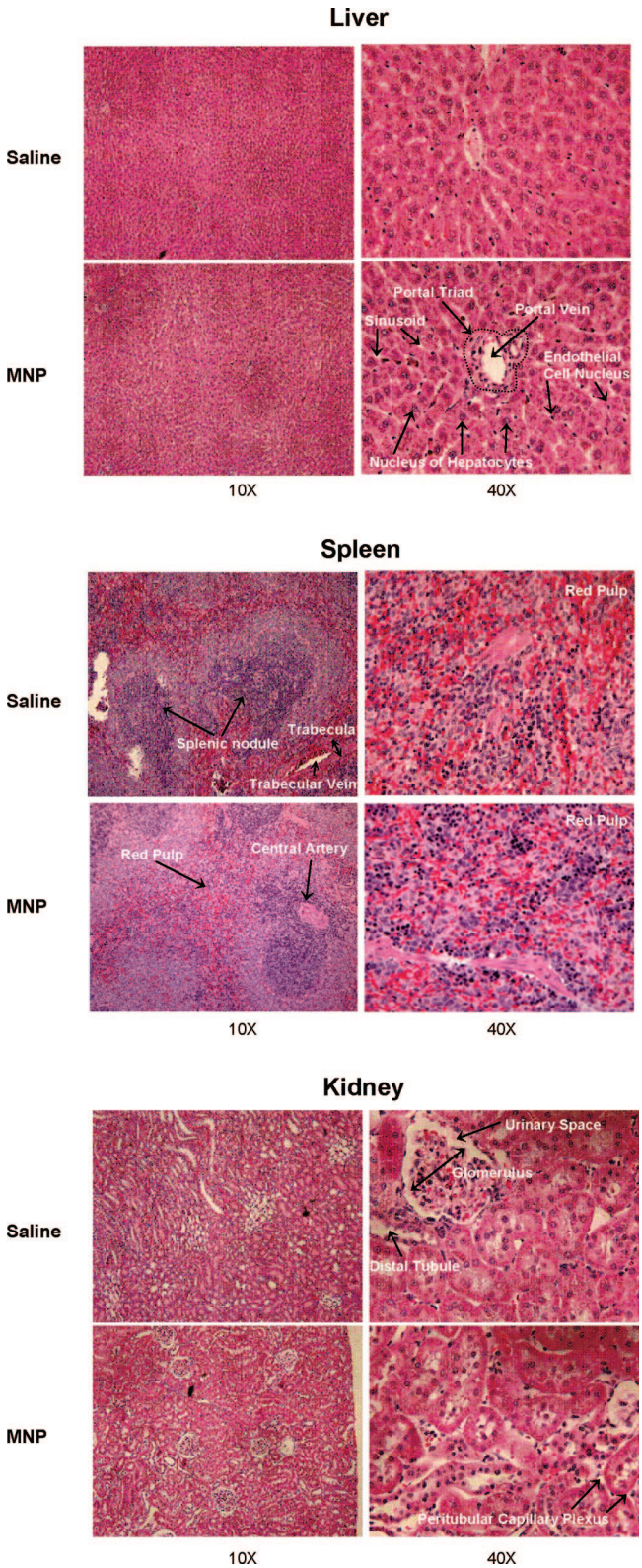

Figure 8. Histological sections of liver, spleen, and kidney samples collected at 1 week following injections of MNPs. Sections were stained with H&E and observed under a light microscope at 10× and 40× magnification.

The increase in iron levels seen particularly in heart and brain at later time points (Figure 3) could be due to the iron released from the degraded MNPs and carried by transferrin. Transferrin is a main iron-binding protein and serves as the transport system of iron to various body cells and tissues. Iron levels in different body compartments at later time points are perhaps controlled by the relative expression of transferrin receptors. In our study, the lack of any change in brain iron levels during the first week after particle injection suggests that the intact MNPs do not cross the blood−brain barrier (BBB). The gradual increase observed at the later time points (Figure 3) could be due to iron binding to transferrin and then being transported across the BBB, as transferrin receptors are overexpressed in brain endothelial cells.[34] The increase in iron content in the brain could be a concern, although it has been reported that free iron, not transferrin-bound iron, causes toxicity.[35] Furthermore, Kim et al.[36] demonstrated no change in the permeability of BBB or immunohistological changes in the brain of mice following intraperitoneal administration of silica-coated 50 nm diameter iron oxide MNPs. We did not notice any behavioral changes in injected animals during the experimental period, suggesting that the slight increase in brain iron levels may not have any toxic effects on the central nervous system.

Similar to our results, Qian et al.[37] also observed an increase in iron levels in rat heart in animals fed with high-iron diets. This increase could be accounted for by the ability of heart cells to accumulate transferrin and nontransferrin-bound iron. The increase in iron levels in liver at later time points could be due partly to the intraportal transport of free iron released from biodegraded MNPs or smaller-sized particles formed as a result of degradation in the spleen.[28,29] Overall, our results demonstrate that the biodistribution of iron is time dependent. The initial biodistribution is primarily controlled by the particle characteristics and at later time points by the iron transport proteins such as transferrin and the affinity of the iron-bound transport protein to different tissues and the level of expression of transferrin receptors. Aging of the animals during the 3-week experimental period might partly explain the increase in iron levels in different tissues over time, but this increase is marginal and ranges

(33) Schulze, E.; Ferrucci, J. T. Jr.; Poss, K.; Lapointe, L.; Bogdanova, A.; Weissleder, R. Cellular uptake and trafficking of a prototypical magnetic iron oxide label in vitro. *Invest. Radiol.* **1995**, *30*, 604–610.

(34) Descamps, L.; Dehouck, M. P.; Torpier, G.; Cecchelli, R. Receptor-mediated transcytosis of transferrin through blood-brain barrier endothelial cells. *Am. J. Physiol. Heart Circ. Physiol.* **1996**, *270*, H1149–H1158.

(35) Gaasch, J. A.; Lockman, P. R.; Geldenhuys, W. J.; Allen, D. D.; Van der Schyf, C. J. Brain iron toxicity: differential responses of astrocytes, neurons, and endothelial cells. *Neurochem. Res.* **2007**, *32*, 1196–1208.

(36) Kim, J. S.; Yoon, T.-J.; Yu, K. N.; Kim, B. G.; Park, S. J.; Kim, H. W.; Lee, K. H.; Park, S. B.; Lee, J.-K.; Cho, M. H. Toxicity and Tissue Distribution of Magnetic Nanoparticles in Mice. *Toxicol. Sci.* **2006**, *89*, 338–347.

(37) Qian, Z. M.; Chang, Y. Z.; Leung, G.; Du, J. R.; Zhu, L.; Wang, Q.; Niu, L.; Xu, Y. J.; Yang, L.; Ho, K. P.; Ke, Y. Expression of ferroportin1, hephaestin and ceruloplasmin in rat heart. *Biochim. Biophys. Acta* **2007**, *1772*, 527–532.

from 2 to 5% per month, depending upon the tissue.[38] To obtain complete biodistribution data including elimination through urine and stools, one can use ^{59}Fe to synthesize iron oxide nanoparticles to achieve greater sensitivity of detection.[39]

The transient increase in ALT, AST, and AKP levels in serum upon administration of MNPs appears to be the general response of the body as PLGA nanoparticles also induced a similar response (Figure 5). It appears that the surge in enzyme activities seen in the animals during the initial days following nanoparticle injection is partly the effect of the anesthetic agent used prior to injection, as a saline injection also caused an increase in the liver AST level (Figure 6). It is known that ketamine−xylazine increases liver enzyme activity and enzymes remain elevated over several hours;[40] however, phenobarbital (used for euthanasia) did not affect liver enzyme activity. Jiang et al.[41] also observed a transient increase in ALT and AST activity following injection of chitosan− and polyethylenimine−DNA complexes. Generally, AST levels three times the upper limit of the normal range (range 39–262 U/L) represent abnormal liver function.[42] The changes seen in our studies were significantly below this limit (Figure 6).[43]

The effect of MNPs on oxidative stress is an important consideration for their safe use in patients. Although iron is present in the body, mostly associated with hemoglobin,[44] previous studies have reported an increase in oxidative stress with an increase in free iron.[45,46] Therefore, usually iron oxide particles are surrounded by different polymeric coatings to prevent direct contact of iron oxide with inter or intracellular substrates that can facilitate free-radical generation.[47] Iron-induced oxidative injury to phospholipids of organelle membranes is a potential mechanism underlying cellular injury in iron overload. We observed a transient increase in LHPO levels in different tissues (Figure 7); however, the response varied from tissue to tissue and does not seem to correlate with the increase in iron levels. For example, liver showed a marginal increase in oxidative stress despite greater localization of iron compared with other tissues. This observation suggests that the oxidative response depends on the capacity of individual tissues to neutralize the effect of stress conditions caused by the particulate injection. Given its main role in detoxification, the liver is exposed to many sources of oxidative stress and may have a greater capacity to neutralize these effects. It appears that nonmagnetic nanoparticles also induce oxidative stress. For example, the uptake of polymeric nanoparticles (poly(isobutyl cynoacrylate)) by Küpffer cells in the liver following intravenous administration induced modifications in the hepatocyte antioxidant system, such as depletion of glutathione or superoxide dismutase, but the events were reversible.[48] The transient increase in the liver enzyme levels or increase in oxidative stress does not seem to be high enough to damage the liver. This is evident from the lack of significant change in the serum TIBC (Figure 2), which is used as an indirect marker for liver function since transferrin is produced in the liver. Changes in the LHPO levels were transient in our studies, and there were no apparent changes in the histology of the liver and other tissues (Figure 8), both of which suggest that the transient increase in oxidative stress does not affect cellular integrity and tissue morphology.

The increase in iron levels observed in some organs could be significantly below toxic levels considering that the dose used is significantly lower than the total body iron content. For example, cirrhosis and hepatocellular carcinoma can develop if the liver iron concentration exceeds 4000 μg/g wet weight.[49,50] In our studies, the liver iron level prior to MNP injection was 123 $\pm$ 23 μg/g wet weight, which did not exceed 300 μg/g following MNP injection at any time during the 3-week experimental period. Further, the dose of iron used in this study is four times the dose that is usually used in humans for imaging applications (2.6 vs 10 mg/kg). Hence, at lower doses, the increase in iron levels or change in oxidative stress or liver enzyme levels will be significantly

(38) Cook, C. I.; Yu, B. P. Iron accumulation in aging: modulation by dietary restriction. *Mech. Ageing Dev.* **1998**, *102*, 1–13.
(39) Tiefenauer, L. X.; Tschirky, A.; Kuhne, G.; Andres, R. Y. In vivo evaluation of magnetite nanoparticles for use as a tumor contrast agent in MRI. *Magn. Reson. Imaging* **1996**, *14*, 391–402.
(40) Thompson, J. S.; Brown, S. A.; Khurdayan, V.; Zeynalzadedan, A.; Sullivan, P. G.; Scheff, S. W. Early effects of tribromoethanol, ketamine/xylazine, pentobarbitol, and isoflurane anesthesia on hepatic and lymphoid tissue in ICR mice. *Comp. Med.* **2002**, *52*, 63–67.
(41) Jiang, X.; Dai, H.; Leong, K. W.; Goh, S. H.; Mao, H. Q.; Yang, Y. Y. Chitosan-g-PEG/DNA complexes deliver gene to the rat liver via intrabiliary and intraportal infusions. *J. Gene Med.* **2006**, *8*, 477–487.
(42) Dufour, D. R. Liver Disease. In *Tietz textbook of clinical chemistry and molecular diagnostics*, 4th ed.; Burtis, C. A., Ashwood, E. R., Bruns, D. E., Eds.; Elsevier Saunders: St. Louis, MO, 2006; 1777−1848.
(43) Olfert, E. D., Cross, B. M., McWilliam, A. A., Eds. *Guide to the Care and Use of Experimental Animals*, 2nd ed.; Canadian Council on Animal Care: Ottawa, 1993.
(44) Puntarulo, S. Iron, oxidative stress and human health. *Mol. Aspects Med.* **2005**, *26*, 299–312.
(45) Mehta, S. H.; Webb, R. C.; Ergul, A.; Tawak, A.; Dorrance, A. M. Neuroprotection by tempol in a model of iron-induced oxidative stress in acute ischemic stroke. *Am. J. Physiol. Regul. Integr. Comp. Physiol.* **2004**, *286*, R283–R288.
(46) Minotti, G. Sources and role of iron in lipid peroxidation. *Chem. Res. Toxicol.* **1993**, *6*, 134–146.
(47) Stroh, A.; Zimmer, C.; Gutzeit, C.; Jakstadt, M.; Marschinke, F.; Jung, T.; Pilgrimm, H.; Grune, T. Iron oxide particles for molecular magnetic resonance imaging cause transient oxidative stress in rat macrophages. *Free Radic. Biol. Med.* **2004**, *36*, 976–984.
(48) Fernandez-Urrusuno, R.; Fattal, E.; Feger, J.; Couvreur, P.; Therond, P. Evaluation of hepatic antioxidant systems after intravenous administration of polymeric nanoparticles. *Biomaterials* **1997**, *18*, 511–517.
(49) Anthony, S.; Tavill, B. R. B. Hemochromatosis: How much iron is too much. *Hepatology* **1986**, *6*, 142–145.
(50) Bassett, M. L.; Halliday, J. W.; Powell, L. W. Value of hepatic iron measurements in early hemochromatosis and determination of the critical iron level associated with fibrosis. *Hepatology* **1986**, *6*, 24–29.

lower than those observed in our study. Bourrinet et al.,[25] in their study with ferumoxtran-10, reported no treatment-associated changes in cardiovascular and renal functions following intravenous injections of 2–20 mg Fe/kg in dogs. Only the high dose (200 mg of Fe/kg), which is 75 times the intended human dose, caused slight and transient changes in hematological parameters and cardiac functions. Hence, the dose and the dosing interval could be critical in preventing MNP-associated damage to tissues.

Conclusions

It appears that the biodistribution of iron and its clearance depends upon simultaneous complex events, and hence the dynamics of iron concentration in different tissues changes with time. Since the iron dose of the MNPs was many times lower than body iron levels, we speculate that the injected iron would be easily metabolized and regulated by the body's normal physiological iron homeostatic mechanisms. The most important result is that the injected iron did not cause long-term changes in liver enzyme levels or oxidative stress, with most of the changes being transient. The anticipated use of MNPs for imaging or drug delivery would not involve repeated dosing over a short time interval, which would allow the body to return to its normal state after the initial transient changes. Future studies, aimed at minimizing the initial RES uptake of MNPs by selecting appropriate Pluronic or PEG for surface modification, could increase the MNP half-life in the blood, which in turn could improve drug targeting and imaging applications of the MNP formulation for targets other than the liver. Given the many studies of MNPs for use in biomedical applications, understanding the biodistribution, elimination, and oxidative stress caused by the MNPs is critical to the successful development of MNPs in the clinical setting.

Acknowledgment. The study reported here is funded by Grant No. R01 EB005822 from the National Institute of Biomedical Imaging and Bioengineering of the National Institutes of Health (to V.L.). We also gratefully acknowledge the gift of Pluronic F-127 from BASF Corp. (Mt. Olive, NJ). We thank Ms. Melissa Jedlicka for proofreading the manuscript.

MP7001285